IKR Publishers

IKR Journal of Multidisciplinary Studies (IKRJMS)
Journal homepage: https://ikrpublishers.com/ikrjms/
Volume-2, Issue-6 (November-December) 2026
OPEN ACCESS
ISSN: 3107-3999 (Online)

# CALPHAD, Thermodynamics, Molecular Modeling, and First-Principles Methods for Metallurgical Slags: From Atomic-Scale Structure to Phase Equilibria and Process Prediction

**Antonio Clareti Pereira, PhD***
PhD in Chemical Engineering, University of São Paulo (USP), Belo Horizonte, Minas Gerais, Brazil

***DOI:*** *10.5281/zenodo.24113850*

**ARTICLE INFO**

***Article history:***
***Received : 23-10-2026***
***Accepted : 03-11-2026***
***Available online : 10-11-2026***

**Copyright © 2026 The Author(s):** This is an open-access article distributed under the terms of the Creative Commons Attribution-NonCommercial **4.0 International License (CC BY-NC 4.0),** which permits non-commercial use, sharing, and reproduction in any medium, provided the original author(s) and source are appropriately credited.

**Citation:** Pereira, A. C. (2026). CALPHAD, Thermodynamics, Molecular Modeling, and First-Principles Methods for Metallurgical Slags: From Atomic-Scale Structure to Phase Equilibria and Process Prediction. *IKR Journal of Multidisciplinary Studies (IKRJMS), 2*(6), 1-18.

**ABSTRACT** **Original Research Article**

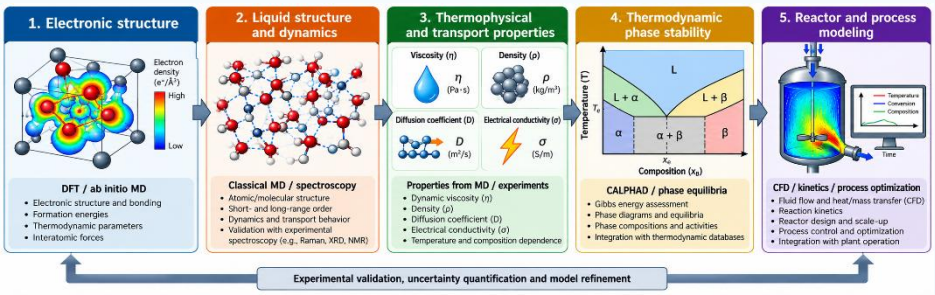
Metallurgical slags simultaneously govern chemical partitioning, heat and mass transfer, refractory interactions, and the separation of valuable metals from oxide phases. Although the CALPHAD (CALculation of PHAse Diagrams) method predicts phase stability and chemical driving forces, its conventional application does not resolve short-range liquid structure or transport kinetics. Conversely, density functional theory (DFT), ab initio molecular dynamics (AIMD), and classical molecular dynamics (MD) can interrogate bonding and liquid networks but cannot independently establish industrial multicomponent equilibria. This critical narrative review examines how these approaches connect across length and time scales, emphasizing thermodynamic descriptions of complex oxide melts, slag structural descriptors, structure–property relationships, experimental validation, and uncertainty-aware process prediction. A section-specific bibliographic framework spans predominantly 2020–2026 literature, supplemented by methodological foundations. The synthesis distinguishes experimentally constrained prediction from plausible but unvalidated scale coupling. It identifies database coverage, redox-dependent speciation, force-field transferability, kinetic departures from equilibrium, and uncertain plant boundary conditions as principal barriers. A staged workflow is proposed in which experimental observations constrain atomistic and thermodynamic models, prediction intervals are tested against unseen conditions, and calibrated outputs inform reactor-scale decisions. Multiscale slag engineering is therefore better viewed as a traceable sequence of validated information transfers than as the simple juxtaposition of modeling techniques.

**Keywords:** CALPHAD, Metallurgical Slags, Molecular Dynamics, First-Principles Calculations, Phase Equilibria, Multiscale Modeling.

### Highlights

- Thermodynamic and atomistic approaches address complementary slag behavior.
- Network topology connects melt composition to transport response.
- Cross-scale predictions require experimental constraints and uncertainty bounds.
- Industrial deployment must account for kinetics and variable feed chemistry.

### Graphical Abstract



*Corresponding author: Antonio Clareti Pereira, PhD
PhD in Chemical Engineering, University of São Paulo (USP), Belo Horizonte, Minas Gerais, Brazil

## Introduction

Metallurgical slags are chemically active oxide liquids, not passive waste streams. Their liquidus temperature, oxidation state, dissolution capacity, viscosity, and phase relations influence metal recovery, impurity removal, slag foaming, furnace integrity, and product quality. A single bulk-basicity index cannot uniquely represent the effects of cation coordination, polymerization, volatile species, or locally different oxygen potentials. Figure 1 outlines the distinct information required for a predictive design workflow, while Table 1 compares the scope of its constituent methods.

This critical narrative review asks when DFT calculations, AIMD simulations, and CALPHAD assessments can yield mutually reinforcing constraints for industrial slag prediction. The bibliographic corpus was selected for topical coverage and emphasizes studies from 2020–2026 alongside methodological foundations. Because full systematic search and exclusion logs are unavailable, no Preferred Reporting Items for Systematic Reviews and Meta-Analyses (PRISMA)-style systematic-review claim is made.

The central distinction is between a thermodynamically admissible state and a state actually achieved within a finite residence time. Equilibrium minimization defines a reference outcome; liquid connectivity and transport influence how rapidly it might be approached, and reactor conditions determine whether the reference is operationally relevant. This distinction informs the structure of the review and the comparison of evidence discussed in Figures 2–4.

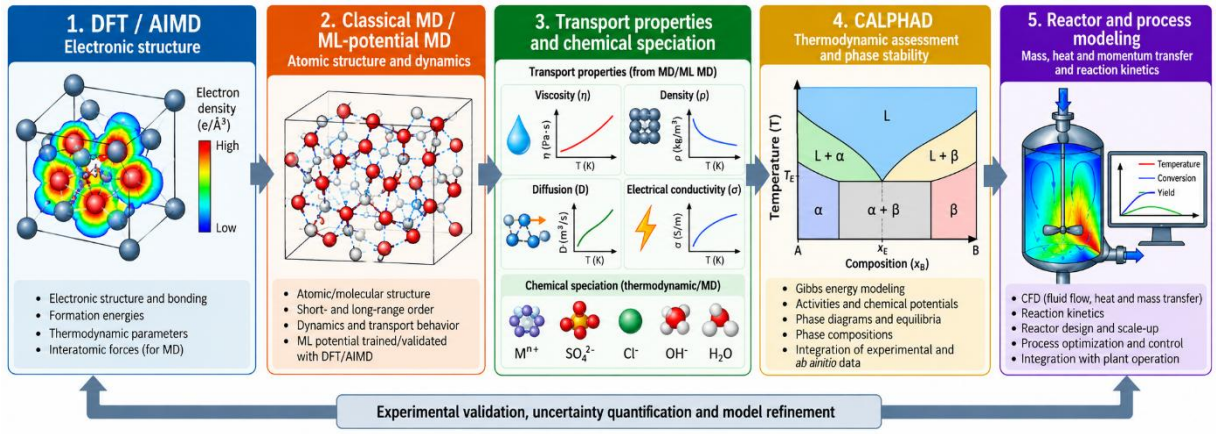



**Figure 1.** Complementary information domains and potential scale-to-scale handoffs.

*Note.* Conceptual diagram prepared for this review; verification of figure provenance and author approval is required before submission. Arrows represent information transfer, not a validated end-to-end workflow. ML = machine learning.

The arrows in Figure 1 should not be interpreted as an automatic coupling algorithm: different uncertainty structures and calibration datasets must be reconciled at every interface.

**Table 1.** Complementary modeling domains for complex oxide slags

| Method | Validated contribution | Main limitation |
|---|---|---|
| **DFT / AIMD** | Bonding, local energetics, redox and short-time dynamics | Functionals, simulation cell size, and temperature sampling |
| **Classical / ML molecular dynamics** | Network descriptors and transport trends | Potential validity and accessible time scales |
| **CALPHAD** | Activities, equilibrium phases, and stable compositions | Database coverage and equilibrium assumption |
| **CFD / kinetic models** | Spatial gradients and transient response | Closure relations and boundary-condition uncertainty |

*Note.* Qualitative synthesis; applicability depends on temperature, composition, oxygen potential, and experimental coverage.

Table 1 establishes why no single method resolves both atomic coordination and plant-scale separation efficiency. The validity domain of each method matters more than its nominal complexity.

This narrative review distinguishes application-specific experimental evidence, atomistic interpretations, thermodynamic assessments, and conceptual proposals. The

evidence classes are not automatically interchangeable, and the scope of any extrapolation should be explicitly identified.

## Thermodynamic Foundations of Metallurgical Slags

The governing criterion for equilibrium is minimization of total Gibbs energy subject to elemental balances and specified temperature, pressure, and exchange potentials. Activities translate composition into chemical potential, $\mu_i = \mu_i^\circ + RT \ln a_i$, and nonideality enters through activity coefficients and composition-dependent interaction terms. Oxide melts require explicit attention to the reference states used for oxide constituents and to the partition between ionic species and structurally meaningful entities.

Oxygen potential links gas chemistry, $Fe^{2+}/Fe^{3+}$ speciation, and the stability of spinel and other solid phases. Calculated metal partitioning may change substantially with imposed $pO_2$ or $pSO_2$ even when bulk oxide composition is unchanged. Basicity and network polymerization influence properties but must not be used as interchangeable substitutes for chemical potential or rigorous Gibbs-energy functions.

A rigorous interpretation separates equilibrium constraints from reaction pathways, interfacial resistances, and gas–slag transport. Observed departures from calculated partitioning may reflect insufficient equilibration, measurement uncertainty, or a genuinely inadequate thermodynamic model; each requires different corrective experiments.

## Thermodynamic Models for Oxide Slags

Ideal, regular, and subregular solution models provide increasingly flexible expressions for excess Gibbs energy but may be poorly suited to melts with strong short-range ordering and changing coordination environments. Associate and ionic descriptions introduce a more explicit representation of interactions, whereas the Modified Quasichemical Model emphasizes pairwise ordering and composition-dependent short-range interactions.

Compound Energy Formalism represents sublattice occupancy and defect chemistry in phases where crystallographic or ionic constraints are justified. Model choice must follow the types and ranges of available observations, not simply mathematical flexibility: an attractive fit to a ternary section may conceal unreliable multicomponent extrapolation.

Two thermodynamic databases can predict different phase boundaries because of different assessments, phase descriptions, standard states, or parameter-optimization strategies. A cross-database comparison should disclose versions, selected solution phases, suppressed phases, and constraints; mere agreement between software packages is not independent validation.

## CALPHAD Assessment of Slag Systems

An assessment is a constrained inversion problem: phase equilibria, activities, calorimetric measurements, and liquidus observations are reconciled through parameterized Gibbs-energy descriptions. Binary parameter quality is necessary but not sufficient for robust ternary and higher-order prediction. Extrapolation reliability depends on the presence of higher-order interactions, consistency across assessed subsystems, and exclusion of incompatible datasets.

Assessment practice should disclose measurement origins and estimated uncertainty, optimization targets, weighting strategy, parameter correlations, and blind validation against data not used for calibration. Figure 2 depicts the distinction between fitting and genuine prediction.

FactSage, Thermo-Calc, and pycalphad provide different software interfaces and model/database ecosystems; results are not directly comparable without specifying database releases and phase selections. Assessment reports should expose numerical solver behavior near miscibility gaps or competing oxide solids rather than presenting a single equilibrium output as a unique experimental fact.

Figure 2 separates source-data assimilation from out-of-sample prediction; an assessment can pass through the first three stages without meeting the fourth.

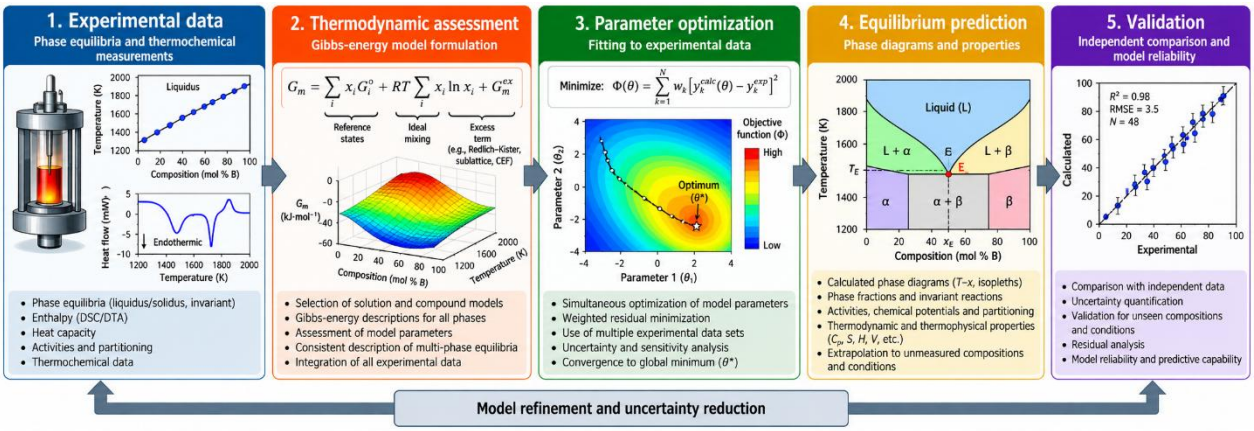



**Figure 2.** Thermodynamic assessment cycle and the independent validation requirement.

*Note.* Conceptual diagram prepared for this review; verification of figure provenance and author approval is required before submission. Arrows represent information transfer, not a validated end-to-end workflow. Gibbs-energy assessment refers to model calibration based on experimental observations.

The essential test is whether fitted Gibbs-energy descriptions transfer to measurements excluded from the parameter-optimization step.

These assessments and tools address different parts of phase-equilibrium inversion, ranging from liquidus constraints to database development and testing. Evaluate their applicability at matched composition and oxygen potential.

A useful distinction in the literature on phase and CALPHAD is between the quantity directly constrained by a method and the process variable ultimately sought. The cited works span related compositions or techniques, yet their contributions should not be treated as a common validated prediction without matched temperature, composition, and reference states (Otis et al., 2017).

For calibration, comparisons must retain the system boundaries and the observables involved. Literature in this group provides potentially complementary methodological or material-specific context; evidence of transfer to more complex industrial slags requires a separate test rather than a title-level analogy (Shishin et al., 2013).

## CALPHAD for Industrial Slag Chemistry

Iron-rich silicate, calcium aluminosilicate, and chromium- or titanium-bearing slags demonstrate why industrial prediction requires chemical boundaries that extend beyond major oxide percentages. Copper smelting combines matte, metal, oxide liquid, spinel, and controlled sulfur–oxygen atmospheres; steelmaking adds phosphorus distribution and fluctuating FeO activity; ferroalloy slags introduce multivalent chromium and complex spinel precipitation.

Slag composition is frequently reported on an oxide basis even though process-relevant components can change valence, transfer between phases, or volatilize. For comparative interpretation, equilibrium calculations should identify all gas, metal, matte, solid, and slag phases and the imposed elemental inventories; otherwise, apparently similar basicity values can describe fundamentally different systems.

Operational merit cannot be inferred from an equilibrium phase diagram alone. A liquidus decrease may improve fluidity but alter refractory compatibility; increased impurity capacity may require an oxygen potential that changes metal losses. Such conflicts should be evaluated as constrained multi-objective design problems, not single-number optima.

Industrial cases should be compared based on feed composition, controlled oxygen and sulfur potentials, competing solid phases, and residence time. Such differences limit direct transfer of operating conclusions among furnaces.

A useful distinction in the literature on metal partitioning is between the quantity directly constrained by a method and the process variable ultimately sought. The cited works span related compositions or techniques, yet their contributions should not be treated as a common validated prediction without matched temperature, composition, and reference states (Chen et al., 2019).

For phase and phosph, comparisons must retain the system boundaries and the observables involved. Literature in this group provides potentially complementary methodological or material-specific context; evidence of transfer to more complex industrial slags requires a separate test rather than a title-level analogy (Gao et al., 2020).

An important unresolved question for phase and oxygen is how well the reported modeling or experimental domain overlaps with industrial operating conditions. These sources inform that question, but generalization requires explicit phase selection, independent measurement, and uncertainty assessment (Hidayat et al., 2018).

Within sulf, the literature is best interpreted in terms of a chain of constraints, not interchangeable model outputs. Assess each contribution against its native experimental or computational conditions before using it to justify process-scale inference (Liu et al., 2021).

A useful distinction in the literature on phase and oxygen is between the quantity directly constrained by a method and the process variable ultimately sought. The cited works span related compositions or techniques, yet their contributions should not be treated as a common validated prediction without matched temperature, composition, and reference states (Nikolic et al., 2010).

For phase and oxygen, comparisons must retain the system boundaries and the observables involved. Literature in this group provides potentially complementary methodological or material-specific context; evidence of transfer to more complex industrial slags requires a separate test rather than a title-level analogy (Peng et al., 2020).

An important unresolved question for industrial applications is how well the reported modeling or experimental domain overlaps with conditions of industrial operation. These sources inform that question, but generalization requires explicit phase selection, independent measurement, and uncertainty assessment (Pereira, 2026c).

Within refract and industrial contexts, the literature is best interpreted as a chain of constraints, not interchangeable model outputs. Assess each contribution against its native experimental or computational conditions before using it to justify process-scale inference (Sineva et al., 2022).

A useful distinction in the literature on phase and refract is between the quantity directly constrained by a method and the process variable ultimately sought. The cited works span related compositions or techniques. However, their contributions should not be treated as a common validated prediction without matched temperature, composition, and reference states (Sun et al., 2020b).

For phase and phosph, comparisons must retain the system boundaries and the observables involved. Literature in this group provides potentially complementary methodological or material-specific context; evidence of transfer to more complex industrial slags requires a separate test rather than a title-level analogy (Sun et al., 2022a).

An important unresolved question for phosph and sulf is how well the reported modeling or experimental domain overlaps with conditions of industrial operation. These sources inform that question, but generalization requires explicit phase selection, independent measurement, and uncertainty assessment (Talapaneni et al., 2018).

Within phase, the literature is best interpreted in terms of a chain of constraints, not interchangeable model outputs. Assess each contribution against its native experimental or computational conditions before using it to justify process-scale inference (Tian et al., 2022).

A useful distinction in the literature on phase is between the quantity directly constrained by a method and the process variable ultimately sought. The cited works span related compositions or techniques, yet their contributions should not be treated as a common validated prediction without matched temperature, composition, and reference states (Wang et al., 2025).

For phase and phosph, comparisons must retain the system boundaries and the observables involved. Literature in this group provides potentially complementary methodological or material-specific context; evidence of transfer to more complex industrial slags requires a separate test rather than a title-level analogy (Xie et al., 2024).

An important unresolved question for phase is how well the reported modeling or experimental domain overlaps with industrial operating conditions. These sources inform that question, but generalization requires explicit phase selection, independent measurement, and uncertainty assessment (Xie et al., 2021).

## Molecular Dynamics of Molten Slags

Classical MD integrates atomic motions using a prescribed interatomic potential, enabling exploration of liquid structure in larger systems and over longer timescales than typical ab initio simulations. Born–Mayer–Huggins and Buckingham forms capture selected repulsive and dispersive interactions, but transferability across valence changes and chemically dissimilar oxide networks remains nontrivial.

Radial distribution functions, coordination numbers, bridging and non-bridging oxygens, and $Q^n$ distributions (where n is the number of bridging oxygens per network-forming tetrahedron) quantify local and intermediate-range structure. These observables depend on counting conventions, cutoff radii, temperature, composition, and the potential model. Structural agreement alone does not establish transport accuracy, particularly where viscosity depends on rare cooperative rearrangements.

Learned potentials may bridge some atomistic scale gaps, provided training data represent high-temperature liquids, mixed valence, and unusual coordination states. Extrapolation diagnostics and independent liquid-state validation are essential to prevent a low test error on crystalline training configurations from masquerading as slag performance.

Molecular simulations of oxide liquids explore network connectivity and local ionic environments across distinct compositional families. Differences in force fields and structural descriptors prevent automatic quantitative comparison.

A useful distinction in the literature on molecules and structure is between the quantity directly constrained by a method and the process variable ultimately sought. The cited works span related compositions or techniques, yet their contributions should not be treated as a common validated prediction without matched temperature, composition, and reference states (Car, 2016).

For molecular comparisons, comparisons must retain the system boundaries and the observables involved. Literature in this group provides potentially complementary methodological or material-specific context; evidence of transfer to more complex industrial slags requires a separate test rather than a title-level analogy (Diao et al., 2017).

An important unresolved question for phosph and molecular is how well the reported modeling or experimental domain overlaps with industrial operating conditions. These sources inform that question, but generalization requires explicit phase selection, independent measurement, and uncertainty assessment (Fan et al., 2015).

Within molecular and structural studies, the literature is best interpreted in terms of a chain of constraints, not interchangeable model outputs. Assess each contribution against its native experimental or computational conditions before using it to justify process-scale inference (Feng et al., 2021).

A useful distinction in the literature on phosph and sulf is between the quantity directly constrained by a method and the process variable ultimately sought. The cited works span related compositions or techniques, yet their contributions should not be treated as a common validated prediction without matched temperature, composition, and reference states (He et al., 2022).

For molecular and structural comparisons, comparisons must retain the system boundaries and the observables involved. Literature in this group provides potentially complementary methodological or material-specific context; evidence of transfer to more complex industrial slags requires a separate test rather than a title-level analogy (Jiang et al., 2018b).

An important unresolved question for molecular structure is how well the reported modeling or experimental domain overlaps with industrial operating conditions. These sources inform that question, but generalization requires explicit phase selection, independent measurement, and uncertainty assessment (Jiang et al., 2020).

Within diffuse and Raman, the literature is best interpreted in terms of a chain of constraints, not interchangeable model outputs. Assess each contribution against its native experimental or computational conditions before using it to justify process-scale inference (Liu et al., 2024).

A useful distinction in the literature on molecule and structure is between the quantity directly constrained by a method and the process variable ultimately sought. The cited works span related compositions or techniques, yet their contributions should not be treated as a common validated prediction without matched temperature, composition, and reference states (Ma et al., 2021a).

For oxygen and molecule comparisons, comparisons must retain the system boundaries and the observables involved. Literature in this group provides potentially complementary methodological or material-specific context; evidence of transfer to more complex industrial slags requires a separate test rather than a title-level analogy (Sun et al., 2024c).

An important unresolved question for molecul and potent is how well the reported modeling or experimental domain overlaps with conditions of industrial operation. These sources inform that question, but generalization requires explicit phase selection, independent measurement, and uncertainty assessment (Xu et al., 2026).

Within molecular structure, the literature is best interpreted in terms of a chain of constraints, not interchangeable model outputs. Assess each contribution against its native experimental or computational conditions before using it to justify process-scale inference (Yao et al., 2017).

A useful distinction in the literature on molecul and potent is between the quantity directly constrained by a method and the process variable ultimately sought. The cited works span related compositions or techniques, yet their contributions should not be treated as a common validated prediction without matched temperature, composition, and reference states (Zhang et al., 2014).

For molecular and structural comparisons, comparisons must retain the system boundaries and the observables involved. Literature in this group provides potentially complementary methodological or material-specific context; evidence of transfer to more complex industrial slags requires a separate test rather than a title-level analogy (Zhou et al., 2023).

## First-Principles and Ab Initio Methods

DFT can evaluate candidate local bonding configurations, energetics, charge distribution, and relative stability. At the same time, AIMD samples thermally fluctuating configurations with on-the-fly electronic calculations. Such methods are particularly useful for testing local coordination hypotheses and generating reference forces for transferable interatomic potentials.

However, finite cells, limited trajectories, electronic exchange–correlation approximations, strong correlation effects, and competing magnetic or oxidation states constrain the certainty of predictions. An inferred ionic charge is not automatically an experimentally measurable oxidation fraction, and a calculated formation energy is not directly a complete composition-dependent liquid Gibbs energy.

The most credible route from first principles to CALPHAD is to treat calculated energy differences as additional constrained observations with explicit uncertainties, then compare improved assessments with withheld experimental phase relations. Direct parameter transfer without statistical or thermodynamic consistency checks risks overinterpreting atomistic calculations.

Electronic-structure and ab initio approaches provide energetic and structural constraints, but neither alone establishes equilibrium phase fractions in real industrial mixtures.

A useful distinction in the literature on phase is between the quantity directly constrained by a method and the process variable ultimately sought. The cited works span related compositions or techniques, yet their contributions should not be treated as a common validated prediction without matched temperature, composition, and reference states (Jones, 2015).

For molecular comparisons, they must retain the system boundaries and the observables involved. Literature in this group provides potentially complementary methodological or material-specific context; evidence of transfer to more complex industrial slags requires a separate test rather than a title-level analogy (Sun et al., 2015).

## Connecting Atomic Structure With Macroscopic Properties

Viscosity, diffusivity, conductivity, density, interfacial tension, and chemical capacities are linked to oxide-network connectivity but respond differently to species mobility, composition, temperature, and charge compensation. Depolymerization often accompanies reduced viscosity in silicate-rich regions, yet this trend is not universal when amphoteric oxides, crystals, or redox-driven associations compete.

Compare structural metrics such as $Q^n$ and non-bridging oxygen fraction against measured property curves at matched temperature and composition. Correlation is not equivalence: two liquids may display similar average network connectivity but differ in cation dynamics or crystallization kinetics. Figure 3 formalizes the conditional chain from network topology to an industrial response.

For process design, treat transport properties as temperature- and composition-dependent functions with uncertainty. Sulfide and phosphate capacities additionally require consistent gas activities and standard states; solubility and phase partitioning are thermodynamic observables, whereas their achievement depends on kinetics.

Figure 3 illustrates why network descriptions must be combined with macroscopic characterization rather than equated with performance.

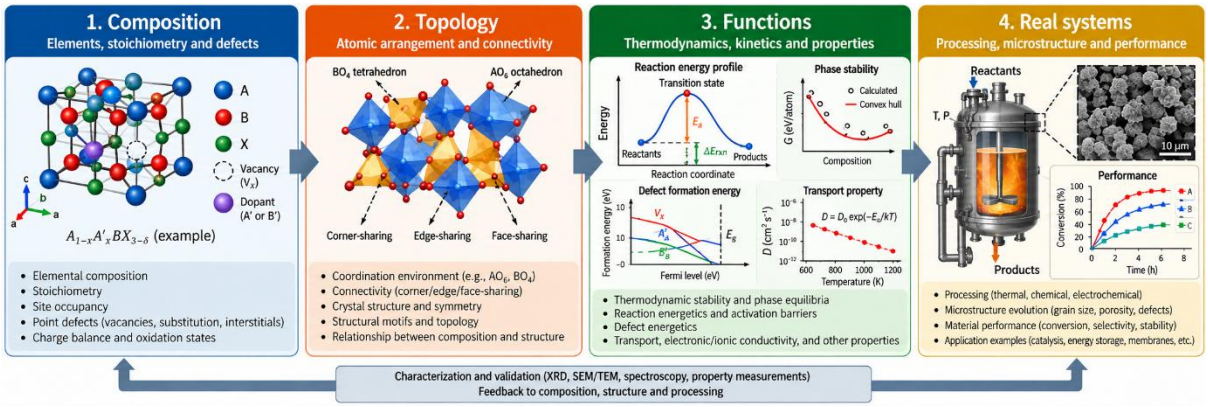



**Figure 3.** Conditional structure–property–process connections in oxide slags.

*Note*. Conceptual diagram prepared for this review; verification of figure provenance and author approval is required before submission. Arrows represent information transfer, not a validated end-to-end workflow. $Q^n$ denotes tetrahedral units with n bridging oxygens; BO = bridging oxygen; NBO = non-bridging oxygen.

Every arrow depends on composition, temperature, and phase state, especially near precipitation boundaries.

The structure–property literature tests whether changes in composition and network connectivity explain viscosity, transport, and interfacial response. Structural interpretation must be qualified by temperature and crystallinity.

A useful distinction in the literature on phosph and molecul is between the quantity directly constrained by a method and the process variable ultimately sought. The cited works span related compositions or techniques, yet their contributions should not be treated as a common validated prediction without matched temperature, composition, and reference states (Fan et al., 2021a).

For viscos and sulf, comparisons must retain the system boundaries and the observables involved. Literature in this group provides potentially complementary methodological or material-specific context; evidence of transfer to more complex industrial slags requires a separate test rather than a title-level analogy (Ju et al., 2019).

An important unresolved question for viscos and molecul is how well the reported modeling or experimental domain overlaps with industrial operating conditions. These sources inform that question, but generalization requires explicit phase selection, independent measurement, and uncertainty assessment (Kovtun et al., 2020).

Within viscos and sulf, the literature is best interpreted in terms of a chain of constraints, not interchangeable model outputs. Assess each contribution against its native experimental or computational conditions before using it to justify process-scale inference (Park et al., 2012).

A useful distinction in the literature on viscos and phosph is between the quantity directly constrained by a method and the process variable ultimately sought. The cited works span related compositions or techniques. Yet, their contributions should not be treated as a common validated prediction without matched temperature, composition, and reference states (Sun et al., 2024b).

For viscos and molecul, comparisons must retain the system boundaries and the observables involved. Literature in this group provides potentially complementary methodological or material-specific context; evidence of transfer to more complex industrial slags requires a separate test rather than a title-level analogy (Wu et al., 2016).

An important unresolved question for viscos and phosph is how well the reported modeling or experimental domain overlaps with conditions of industrial operation. These sources inform that question, but generalization requires explicit phase selection, independent measurement, and uncertainty assessment (Zhao et al., 2026a).

Within viscos and sulf, the literature is best interpreted in terms of a chain of constraints, not interchangeable model outputs. Assess each contribution against its native

experimental or computational conditions before using it to justify process-scale inference (Zuo et al., 2021).

## Multiscale Coupling: DFT, MD, CALPHAD, and Process Models

Coupling must be operationally defined. A one-way workflow might use DFT-derived reference forces to fit a potential, MD to estimate structural or transport trends, CALPHAD to predict phase populations, and reactor calculations to integrate transport and residence-time effects. A bidirectional workflow could use experimentally measured phase chemistry to revise electronic or molecular assumptions.

These layers do not share a universal state description: DFT samples configurations at fixed atom counts, MD resolves trajectories, and CALPHAD minimizes macroscopic free energy. Therefore, mapping an AIMD energy distribution directly to a liquidus temperature or using a single MD viscosity value as a general kinetic closure is unjustified without carefully defined temperature, composition, statistical ensembles, and reference states.

An evidence hierarchy can distinguish (i) separate model applications, (ii) cross-method qualitative consistency, (iii) quantitatively calibrated transfer, and (iv) prediction validated on unseen process conditions. Many attractive integration diagrams demonstrate the first two stages rather than the fourth, and should be labeled accordingly.

An integrated model requires compatible state definitions, explicit uncertainty propagation, and measurable quantities at each handoff, not merely the sequential execution of software packages.

A useful distinction in the literature on potent and learn is between the quantity directly constrained by a method and the process variable ultimately sought. The cited works span related compositions or techniques, yet their contributions should not be treated as a common validated prediction without matched temperature, composition, and reference states (Mishin, 2021).

For potent, comparisons must retain the system boundaries and the observables involved. Literature in this group provides potentially complementary methodological or material-specific context; evidence of transfer to more complex industrial slags requires a separate test rather than a title-level analogy (Thompson et al., 2015).

## Validation Against Experimental Techniques

Equilibration–quenching followed by electron-probe microanalysis constrains phase composition and distribution, while differential thermal analysis and calorimetry support transition temperatures and enthalpies. Raman spectroscopy, Fourier-transform infrared spectroscopy (FTIR), X-ray absorption near-edge structure (XANES), extended X-ray absorption fine structure (EXAFS), neutron scattering, and synchrotron methods provide complementary but model-dependent structural or speciation information. High-temperature in situ approaches reduce quenching-related ambiguities but introduce specialized atmosphere and signal-interpretation challenges.

Experimental datasets should report temperature calibration, oxygen and sulfur potentials, residence and equilibration criteria, quench histories, sampling locations, replicate variability, and, where relevant, mass closure. Without these conditions, comparisons of liquidus, viscosity, or oxidation state can conflate model error with uncontrolled thermochemical boundaries.

Validation should be method-specific. Spectroscopic agreement can support coordination assignments yet not independently prove viscosity; accurate equilibrium phase fractions do not prove kinetics; and a successful viscosity correlation cannot independently identify the correct short-range ordering mechanism. Cross-observable agreement is stronger than agreement against a single fitted endpoint.

Independent experimental constraints are needed at both the structural and thermodynamic levels. Comparisons should distinguish measurements from interpretation and fitted versus withheld observations.

A useful distinction in the literature on viscosity and temperature is between the quantity a method directly constrains and the process variable ultimately sought. The cited works span related compositions or techniques, yet their contributions should not be treated as a common validated prediction without matched temperature, composition, and reference states (Ding et al., 2020).

For phase and viscosity, comparisons must retain the system boundaries and the observables involved. Literature in this group provides potentially complementary methodological or material-specific context; evidence of transfer to more complex industrial slags requires a separate test rather than a title-level analogy (Sineva et al., 2020b).

An important unresolved question for spectroscopic assignment is how well the reported modeling or experimental domain overlaps with industrial operating conditions. These sources inform that question, but generalization requires explicit phase selection, independent measurement, and uncertainty assessment (Sineva et al., 2023).

Within Raman and molecular studies, the literature is best interpreted as a chain of constraints, not interchangeable model outputs. Assess each contribution against its native experimental or computational conditions before using it to justify process-scale inference (Zhou et al., 2022).

## Uncertainty, Model Transferability, and Major Limitations

Uncertainty arises from experimental measurements, model structure, parameter identifiability, software and database versions, phase suppression decisions, and industrial boundary conditions. Even precise numerical minimization can produce misleading certainty when metastable phases, gas release, incomplete mixing, or unrepresented trace components dominate practical outcomes.

MD uncertainty includes force-field transfer, finite size, sampling duration, and incomplete exploration of slow relaxation modes. DFT uncertainty includes electronic approximations, structure selection, temperature corrections, and limited composition ensembles. CALPHAD uncertainty includes correlated parameters and sparse high-order datasets. These terms should not be collapsed into an undocumented single percentage.

A robust transfer test deliberately holds out compositions, temperatures, oxygen potentials, and process scales not used in model calibration. Uncertainty propagation through a process flowsheet should distinguish epistemic uncertainty, reducible by evidence, from aleatory variability in feeds and operations.

The reliability of cross-scale inference rests on uncertainty characterization and transfer tests that include compositions and conditions absent from parameter fitting.

A useful distinction in the literature on phase and uncertainty is between the quantity directly constrained by a method and the process variable ultimately sought. The cited works span related compositions or techniques, yet their contributions should not be treated as a common validated prediction without matched temperature, composition, and reference states (Paulson et al., 2018).

For uncertain comparisons, they must retain the system boundaries and the observables involved. Literature in this group provides potentially complementary methodological or material-specific context; evidence of transfer to more complex industrial slags requires a separate test rather than a title-level analogy (Paulson et al., 2019).

## Emerging Directions and Research Priorities

Machine-learned interatomic potentials, Bayesian assessments, automated thermodynamic optimization, and physics-informed surrogates can accelerate exploration of difficult multicomponent spaces. Their scientific value depends on calibrated uncertainty, informative data selection, and physically credible extrapolation, not merely faster execution or higher dimensionality.

Active learning offers a practical means to target poorly sampled liquid configurations, oxide valence states, or phase boundaries. Bayesian CALPHAD can represent parameter covariance and distribute predictive intervals over phase fields; CFD–CALPHAD and kinetic coupling can translate bounded equilibrium information into transient transport models.

Priority should be given to interoperable datasets with recorded oxygen potential, spectroscopy-assisted speciation, in situ high-temperature observations, public benchmark compositions, withheld validation sets, and pilot-scale reconciliation of heat and elemental balances. Figure 4 illustrates a validation-first deployment pathway.

Figure 4 introduces a staged approach to transferable, auditable predictions.

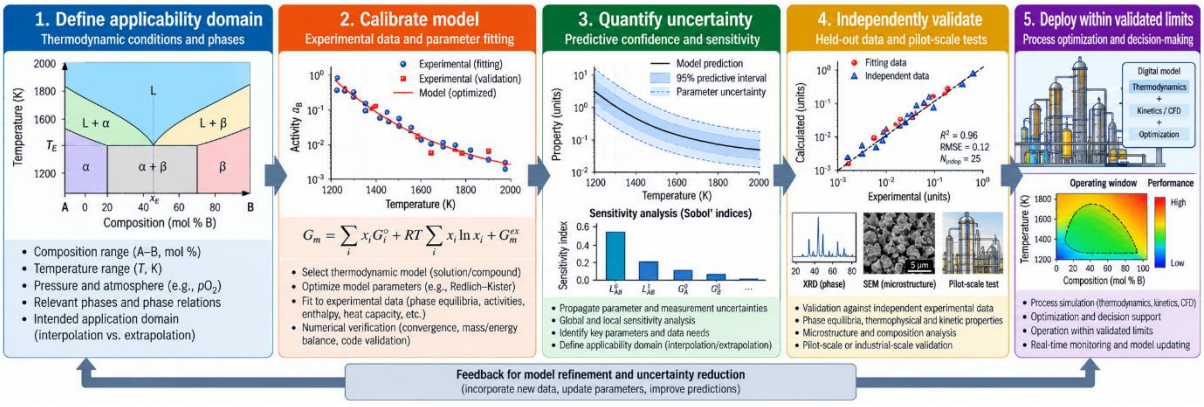



**Figure 4.** Validation-first pathway for uncertainty-aware process applications.

*Note.* Conceptual diagram prepared for this review; verification of figure provenance and author approval is required before submission. Arrows represent information transfer, not a validated end-to-end workflow. UQ = uncertainty quantification; $pO_2$ = oxygen partial pressure.

Process deployment should be conditional on the domain represented by calibration and independent validation, with renewed evaluation when feed chemistry changes.

New surrogate and learning methods can improve computational throughput, although their generalization to

liquid slags remains conditional on training-domain coverage and independent validation.

A useful distinction in the literature on potent and learn is between the quantity directly constrained by a method and the process variable ultimately sought. The cited works span related compositions or techniques, yet their contributions should not be treated as a common validated prediction without matched temperature, composition, and reference states (Behler, 2016).

## Conclusions and Research Priorities

CALPHAD, molecular dynamics, and first-principles methods supply complementary rather than interchangeable descriptions of metallurgical slags. Thermodynamic modeling is strongest in identifying stable phase assemblages and chemical driving forces within assessed domains; atomistic methods are strongest in investigating bonding, liquid topology, and microscopic dynamics. Neither alone guarantees industrial prediction under transient, heterogeneous operating conditions. The key research opportunity is to convert qualitative multiscale compatibility into tested, traceable quantitative handoffs. Priorities are thermodynamically consistent multicomponent databases, experimentally constrained liquid speciation, transferable interatomic models, uncertainty-aware validation, and explicit kinetic and reactor-scale closure. This review proposes the credibility of out-of-sample predictions, rather than the number of connected software tools, as the benchmark for predictive slag engineering.

## Declarations

Funding. To be confirmed by the corresponding author prior to submission.

Conflict of Interest. To be confirmed by the corresponding author prior to submission.

**Data Availability.** No new experimental datasets were generated for this literature-based manuscript; the bibliographic corpus is supplied separately.

**Author Contributions.** Conceptualization, literature synthesis, critical interpretation, writing, and visualization: Antonio Clareti Pereira (subject to author confirmation).

## References

1. Abdeyazdan, H., Shevchenko, M., Hayes, P. C., & Jak, E. (2022). Integrated experimental and thermodynamic study of the PbO-MgO-SiO2 system. Metallurgical and Materials Transactions B, 53, 954–967. https://doi.org/10.1007/s11663-022-02440-6
2. Avarmaa, K., Klemettinen, L., O'Brien, H., Taskinen, P., & Jokilaakso, A. (2019). Critical metals Ga, Ge and In in copper smelting and converting slags. Minerals Engineering, 137, 27–38. https://scholar.google.com/scholar?q=%22Critical+metals+Ga%2C+Ge+and+In+in+copper+smelting+and+converting+slags%22
3. Avarmaa, K., Yliaho, S., Taskinen, P., & Jokilaakso, A. (2020). Trace-element behavior in copper converting and slag-cleaning systems. Metallurgical and Materials Transactions B, 51, 2435–2448. https://scholar.google.com/scholar?q=%22Trace-element+behavior+in+copper+converting+and+slag-cleaning+systems%22
4. Bartók, A. P., Payne, M. C., Kondor, R., & Csányi, G. (2010). Gaussian approximation potentials: The accuracy of quantum mechanics, without the electrons. Physical Review Letters, 104, 136403. https://doi.org/10.1103/PhysRevLett.104.136403
5. Behler, J. (2011). Atom-centered symmetry functions for constructing high-dimensional neural network potentials. The Journal of Chemical Physics, 134, 074106. https://doi.org/10.1063/1.3553717
6. Behler, J. (2016). Perspective: Machine learning potentials for atomistic simulations. The Journal of Chemical Physics, 145, 170901. https://doi.org/10.1063/1.4966192
7. Bi, Z., Jiang, C., Li, K., Zhang, J., Sun, M., & Wang, Z. (2021a). Amphoteric effects of Al2O3 and B2O3 on aluminosilicate slag networks. Ceramics International, 47, 12252–12262. https://doi.org/10.1016/j.ceramint.2021.01.074
8. Bi, Z., Li, K., Jiang, C., Zhang, J., Ma, S., Sun, M., Wang, Z., & Li, H. (2021b). Effects of B2O3 on the structure and properties of blast furnace slag by molecular dynamics simulation. Journal of Non-Crystalline Solids, 551, 120412. https://doi.org/10.1016/j.jnoncrysol.2020.120412
9. Bocklund, B., Otis, R. A., Egorov, A., Obaied, A., Roslyakova, I., & Liu, Z.-K. (2019). ESPEI for efficient thermodynamic database development, modification, and uncertainty quantification: Application to Cu-Mg. MRS Communications, 9, 618–627. https://doi.org/10.1557/mrc.2019.59
10. Burke, K. (2012). Perspective on density functional theory. The Journal of Chemical Physics, 136, 150901. https://doi.org/10.1063/1.4704546
11. Car, R. (2016). Introduction to density-functional theory and first-principles molecular dynamics. Annual Review of Materials Research, 46, 1-25. https://scholar.google.com/scholar?q=%22Introduction+to+density-functional+theory+and+first-principles+molecular+dynamics%22

12. Chen, M., Avarmaa, K., Klemettinen, L., Taskinen, P., & Jokilaakso, A. (2019). Liquid/spinel/matte/gas equilibria in iron silicate slags relevant to copper smelting. Calphad, 66, 101642. https://doi.org/10.1016/j.calphad.2019.101642
13. Chen, M., Avarmaa, K., Taskinen, P., & Jokilaakso, A. (2020). Thermodynamic and experimental analysis of copper-bearing iron silicate slags. Calphad, 69, 101744. https://scholar.google.com/scholar?q=%22Thermodynamic+and+experimental+analysis+of+copper-bearing+iron+silicate+slags%22
14. Chen, M., Avarmaa, K., Taskinen, P., Lindberg, D., & Jokilaakso, A. (2022a). Experimental phase equilibria of FeOx-saturated iron silicate slags and metallic copper alloys at 1200-1300 °C. Calphad, 77, 102418. https://doi.org/10.1016/j.calphad.2022.102418
15. Chen, M., Avarmaa, K., Taskinen, P., Michallik, R., & Jokilaakso, A. (2022b). Investigation of the matte/slag/spinel/gas equilibria in the Cu-Fe-O-S-SiO2-(CaO, Al2O3) system at 1250 °C and pSO2 of 0.25 atm. Mineral Processing and Extractive Metallurgy Review, 44, 313–324. https://doi.org/10.1080/08827508.2022.2047966
16. Chen, Y., Pan, W., Jia, B., Wang, Q., Zhang, X., Wang, Q., & He, S. (2021). Amphoteric behavior of Al2O3 in CaO-SiO2-Al2O3 melts: Molecular dynamics insights. Journal of Non-Crystalline Solids, 552, 120435. https://doi.org/10.1016/j.jnoncrysol.2020.120435
17. Deringer, V. L., Caro, M. A., & Csányi, G. (2019). Machine learning interatomic potentials as emerging tools for materials science. Advanced Materials, 31, 1902765. https://doi.org/10.1002/adma.201902765
18. Diao, J., Fan, G., Liu, X., Zhang, Z., & Xie, B. (2014). Molecular dynamics simulation of molten CaO-SiO2-P2O5 slags. Metallurgical and Materials Transactions B, 45, 1942-1951. https://doi.org/10.1007/s11663-014-0092-1
19. Diao, J., Fan, G., Liu, X., Zhang, Z., & Xie, B. (2017). Structural characteristics of molten CaO-SiO2-P2O5-FeO slag by molecular dynamics simulation. High Temperature Materials and Processes, 36, 871-878. https://doi.org/10.1515/htmp-2016-0054
20. Diao, J., Fan, G., Liu, X., Zhang, Z., & Xie, B. (2018). Transport properties of CaO-SiO2-P2O5-FeO slags from molecular dynamics simulation. High Temperature Materials and Processes, 37, 141-148. https://doi.org/10.1515/htmp-2016-0159
21. Ding, W., Blanpain, B., & Mertens, G. (2020). High-temperature slag structure and viscosity: Experimental and modeling perspectives. Metallurgical and Materials Transactions B, 51, 1701-1715. https://scholar.google.com/scholar?q=%22High-temperature+slag+structure+and+viscosity%3A+Experimental+and+modeling+perspectives%22
22. Dong, J., Li, D., Tian, J., & Jiang, Z. (2025). Atomic ionic-scale mechanism of inclusion modification by calcium treatment in the electroslag remelting process based on ion and molecule coexistence theory and molecular dynamics simulation. ISIJ International, 65(3), 350–359. https://doi.org/10.2355/isijinternational.ISIJINT-2024-335
23. Du, C., Gao, X., Ueda, S., & Kitamura, S.-Y. (2021). Molecular dynamics study of P2O5-based binary melts and phosphate structural units. Journal of Molecular Liquids, 339, 116818. https://doi.org/10.1016/j.molliq.2021.116818
24. Du, C., Gao, X., Ueda, S., & Kitamura, S.-Y. (2022). Effect of CaF2 on microstructure and transport properties of phosphosilicate slags. Materials, 15, 7916. https://doi.org/10.3390/ma15227916
25. Fan, G., Diao, J., Jiang, L., Zhang, Z., & Xie, B. (2015). Molecular dynamics analysis of the microstructure of the CaO-P2O5-SiO2 slag system with varying P2O5/SiO2 ratios. Materials Transactions, 56, 655-660. https://doi.org/10.2320/matertrans.M2014363
26. Fan, H., Xu, Z., Zhu, Y., & Wang, R. (2021a). Effect of B2O3 on titanium-bearing slag structure and transport properties by molecular dynamics. Journal of Materials Research and Technology, 15, 1046-1057. https://doi.org/10.1016/j.jmrt.2021.08.032
27. Fan, H., Zhu, Y., Xu, Z., & Wang, R. (2021b). Molecular dynamics investigation of FeO-TiO2-SiO2 slag structure. Journal of Non-Crystalline Solids, 571, 121049. https://doi.org/10.1016/j.jnoncrysol.2021.121049
28. Fan, H., Zhu, Y., Xu, Z., & Wang, R. (2022). Structure of the TiO2-MgO-Al2O3 system: Insights from molecular dynamics simulations. Journal of Non-Crystalline Solids, 584, 121482. https://doi.org/10.1016/j.jnoncrysol.2022.121482
29. Feng, D., Zhang, J., Jiang, C., Li, K., & Wang, Z. (2021). Effect of B2O3 on CaO-Al2O3-B2O3 melt structure by molecular dynamics simulation. Journal of Non-Crystalline Solids, 574, 121141. https://doi.org/10.1016/j.jnoncrysol.2021.121141
30. Gao, X., Kitamura, S.-Y., & Ueda, S. (2014). In situ observation of phase formation in dephosphorization slags. ISIJ International, 54, 2375–2383. https://scholar.google.com/scholar?q=%22In+situ+observation+of+phase+formation+in+dephosphorization+slags%22
31. Gao, X., Kitamura, S.-Y., & Ueda, S. (2020). Thermodynamics and phase relations for phosphorus partition in steelmaking slags. ISIJ International, 60, 1–12. https://scholar.google.com/scholar?q=%22Thermodynamics+and+phase+relations+for+phosphorus+partition+in+steelmaking+slags%22

32. Gong, W., Lindberg, D., & Taskinen, P. (2020). Thermodynamic modeling of oxygen potential and iron redox in copper smelting slags. Metallurgical and Materials Transactions B, 51, 2290–2303. https://scholar.google.com/scholar?q=%22Thermodynamic+modeling+of+oxygen+potential+and+iron+redox+in+copper+smelting+slags%22
33. Gu, S., Liu, W., Sun, Y., Tan, M., & Li, T. (2023). Molecular dynamics analysis of phosphate cluster evolution in CaO-SiO2-P2O5 melts. Journal of Molecular Liquids, 382, 121912. https://scholar.google.com/scholar?q=%22Molecular+dynamics+analysis+of+phosphate+cluster+evolution+in+CaO-SiO2-P2O5+melts%22
34. Guo, C., Liu, Y., Tan, J., Du, Y., Chen, W., & Deng, T. (2024). Phase equilibria study and thermodynamic assessment of CaO–MgO–P2O5 system. Calphad, 86, 102711. https://doi.org/10.1016/j.calphad.2024.102711
35. Hayes, P. C., Hidayat, T., & Jak, E. (2015). High-temperature equilibration and quenching techniques for complex slag phase equilibria. Journal of Phase Equilibria and Diffusion, 36, 1–12. https://scholar.google.com/scholar?q=%22High-temperature+equilibration+and+quenching+techniques+for+complex+slag+phase+equilibria%22
36. He, S., Wang, Q., Xie, D., & Xu, C. (2019). Molecular dynamics simulation of structure and transport properties of CaO-SiO2-CaF2 slags. Metallurgical and Materials Transactions B, 50, 1503-1512. https://doi.org/10.1007/s11663-019-01547-7
37. He, X., Ma, S., Wang, L., Dong, H., & Chou, K. (2021). An ab initio molecular dynamics simulation of liquid FeO-SiO2 silicate system with sulfur dissolving. Metallurgical and Materials Transactions B, 52, 3346-3353. https://doi.org/10.1007/s11663-021-02263-x
38. He, X., Ma, S., Wang, L., Dong, H., & Chou, K. (2022). Comparison of desulfurization mechanisms in liquid CaO-SiO2 and MnO-SiO2: An ab initio molecular dynamics simulation. Journal of Alloys and Compounds, 896, 163008. https://doi.org/10.1016/j.jallcom.2021.163008
39. Hidayat, T., Fallah-Mehrjardi, A., Hayes, P. C., & Jak, E. (2018). Experimental techniques for high-temperature phase equilibria in complex oxide slag systems. Journal of Phase Equilibria and Diffusion, 39, 615–628. https://scholar.google.com/scholar?q=%22Experimental+techniques+for+high-temperature+phase+equilibria+in+complex+oxide+slag+systems%22
40. Huang, A., Huo, Y., Yang, J., Gu, H., & Li, G. (2020). Computational modeling and prediction of viscosity of slags by big data mining. Minerals, 10, 257. https://doi.org/10.3390/min10030257
41. Huang, W., Persson, K. A., & Ceder, G. (2018). First-principles thermodynamics and phase stability in multicomponent oxides. npj Computational Materials, 4, 1–10. https://scholar.google.com/scholar?q=%22First-principles+thermodynamics+and+phase+stability+in+multicomponent+oxides%22
42. Jiang, C., Li, K., Bi, Z., Ma, S., Zhang, J., Liu, B., & Li, J. (2024). Developments in atomistic and nanostructure evolution mechanisms of molten slag using atomistic simulation methods. Nanomaterials, 14, 464. https://doi.org/10.3390/nano14050464
43. Jiang, C., Li, K., Zhang, J., Bi, Z., Ma, S., Sun, M., & Wang, Z. (2021). Structure-property relationships of multicomponent blast furnace slags by molecular dynamics. Journal of Molecular Liquids, 330, 115650. https://scholar.google.com/scholar?q=%22Structure-property+relationships+of+multicomponent+blast+furnace+slags+by+molecular+dynamics%22
44. Jiang, C., Li, K., Zhang, J., Liu, Z., Sun, M., Wang, Z., & Liang, W. (2018b). Influence of MgO/Al2O3 ratio on blast furnace slag structure by molecular dynamics. Journal of Non-Crystalline Solids, 502, 76–82. https://scholar.google.com/scholar?q=%22Influence+of+MgO%2FAl2O3+ratio+on+blast+furnace+slag+structure+by+molecular+dynamics%22
45. Jiang, C., Li, K., Zhang, J., Qin, Q., Liu, Z., Sun, M., Wang, Z., & Liang, W. (2019). Effect of MgO/Al2O3 ratio on the structure and properties of blast furnace slag: A molecular dynamics study. Metallurgical and Materials Transactions B, 50, 367–375. https://doi.org/10.1007/s11663-018-1450-1
46. Jiang, C., Li, K., Zhang, J., Sun, M., Wang, Z., & Liang, W. (2018a). Effects of CaO and MgO on the structure and properties of aluminosilicate melts by molecular dynamics. Journal of Molecular Liquids, 268, 762–772. https://doi.org/10.1016/j.molliq.2018.07.123
47. Jiang, C., Zhang, H., Xiong, Z., Chen, S., Li, K., Zhang, J., Liang, W., Sun, M., Wang, Z., & Wang, L. (2020). Molecular dynamics investigations on the effect of Na2O on the structure and properties of blast furnace slag under different basicity conditions. Journal of Molecular Liquids, 299, 112195. https://doi.org/10.1016/j.molliq.2019.112195
48. Jones, R. O. (2015). Density functional theory: Its origins, rise to prominence, and future. Reviews of Modern Physics, 87, 897–923. https://doi.org/10.1103/RevModPhys.87.897
49. Ju, J., Liu, W., Xing, X., Wang, J., & An, J. (2019). Sulfide capacity of CaO-SiO2-8%MgO-Al2O3-BaO slags. Metallurgical Research & Technology, 116, 106. https://scholar.google.com/scholar?q=%22Sulfide+capacity+of+CaO-SiO2-8%25MgO-Al2O3-BaO+slags%22

50. Kim, Y., & Park, H. (2019). Estimation of TiO2-FeO-Na2O slag viscosity via molecular dynamics. Scientific Reports, 9, 17338. https://doi.org/10.1038/s41598-019-53961-1
51. Kim, Y., Nam, C., Kim, S., & Jeon, H. (2021). Rheological properties and structure of molten FeO-TiO2-B2O3 ilmenite smelting slag. Journal of Non-Crystalline Solids, 552, 120308. https://doi.org/10.1016/j.jnoncrysol.2020.120308
52. Klemettinen, L., Avarmaa, K., Taskinen, P., O'Brien, H., & Jokilaakso, A. (2020). Distribution behavior of precious and trace elements in copper smelting systems. Metallurgical and Materials Transactions B, 51, 2770–2784. https://scholar.google.com/scholar?q=%22Distribution+behavior+of+precious+and+trace+elements+in+copper+smelting+systems%22
53. Kovtun, O., Korobeinikov, I., Shukla, A. K., Volkova, O., & Scheller, P. R. (2020). Viscosity of BOF slag. Metals, 10, 982. https://doi.org/10.3390/met10070982
54. Lee, Y. E., & Kolbeinsen, L. (2021). Behavior of slag in ferromanganese and silicomanganese smelting. Metallurgical and Materials Transactions B, 52, 3142–3150. https://doi.org/10.1007/s11663-021-02242-2
55. Lejaeghere, K., Bihlmayer, G., Björkman, T., Blaha, P., Blügel, S., Blum, V., Caliste, D., Castelli, I. E., Clark, S. J., Dal Corso, A., de Gironcoli, S., Deutsch, T., Dewhurst, J. K., Di Marco, I., Draxl, C., Dułak, M., Eriksson, O., Flores-Livas, J. A., Garrity, K. F., ... Cottenier, S. (2016). Reproducibility in density functional theory calculations of solids. Science, 351, aad3000. https://doi.org/10.1126/science.aad3000
56. Li, J., Zhou, C., Wang, S., Zhao, J., Ai, L., & Zhao, D. (2022). Molecular dynamics simulation of oxide slag microstructure and diffusion. Materials, 15, 6512. https://scholar.google.com/scholar?q=%22Molecular+dynamics+simulation+of+oxide+slag+microstructure+and+diffusion%22
57. Li, K., Li, H., Jiang, C., Zhang, J., Liu, Z., & Ren, S. (2020). Transferability of interatomic potentials for SiO2-CaO-MgO-Al2O3 melts. Molecular Simulation, 46, 289–299. https://scholar.google.com/scholar?q=%22Transferability+of+interatomic+potentials+for+SiO2-CaO-MgO-Al2O3+melts%22
58. Liang, D., Yan, Z., Lv, X., Zhang, J., & Bai, C. (2017). Structural transition of blast furnace slag from silicate to aluminate network: Molecular dynamics and Raman spectroscopy. Metallurgical and Materials Transactions B, 48, 573–581. https://doi.org/10.1007/s11663-016-0855-y
59. Liao, J., Wang, X., Liu, F., & Zhao, B. (2023). Experimental validation of thermodynamic databases for Ti-bearing metallurgical slags. Calphad, 81, 102575. https://scholar.google.com/scholar?q=%22Experimental+validation+of+thermodynamic+databases+for+Ti-bearing+metallurgical+slags%22
60. Liu, C., Zhang, X., & Jiang, M. (2022b). Structure-based viscosity prediction of silicate slags using molecular dynamics. Ceramics International, 48, 28291–28298. https://doi.org/10.1016/j.ceramint.2022.06.136
61. Liu, W., & Zuo, H. (2021). Effects of MnO and substitution of CaO by BaO on desulfurization of blast furnace slag. Metallurgical and Materials Transactions B, 52, 2275–2282. https://scholar.google.com/scholar?q=%22Effects+of+MnO+and+substitution+of+CaO+by+BaO+on+desulfurization+of+blast+furnace+slag%22
62. Liu, W., Chen, J., Pang, Z., Wang, J., Zuo, H., & Xue, Q. (2022a). Structure and viscosity of BaO-bearing slag by molecular dynamics, Raman and 27Al NMR. Journal of Molecular Liquids, 359, 119342. https://doi.org/10.1016/j.molliq.2022.119342
63. Liu, W., Sun, Y., Tan, M., Li, T., Gu, S., & Ju, L. (2024). Effect of CaO on the ionic microstructure and properties in dephosphorization slag by molecular dynamics simulation. Journal of Molecular Liquids, 395, 123799. https://doi.org/10.1016/j.molliq.2023.123799
64. Liu, W., Xing, X., & Zuo, H. (2020). Effect of TiO2 on viscosity and sulfide capacity of BaO-bearing blast furnace slag. ISIJ International, 60, 1886-1891. https://scholar.google.com/scholar?q=%22Effect+of+TiO2+on+viscosity+and+sulfide+capacity+of+BaO-bearing+blast+furnace+slag%22
65. Lyu, S., Zhang, J., Li, K., Jiang, C., & Bi, Z. (2025). Molecular dynamics simulation of rare-earth-containing aluminosilicate melts. Journal of Molecular Liquids, 416, 127037. https://doi.org/10.1016/j.molliq.2025.127037
66. Ma, S., Jiang, C., Li, K., Zhang, J., Bi, Z., & Sun, M. (2020). Atomic-scale interpretation of basicity effects in aluminosilicate slags. Journal of Non-Crystalline Solids, 545, 120235. https://scholar.google.com/scholar?q=%22Atomic-scale+interpretation+of+basicity+effects+in+aluminosilicate+slags%22
67. Ma, S., Li, K., Zhang, J., Jiang, C., Bi, Z., Sun, M., & Wang, Z. (2021a). Effect of MnO content on slag structure and properties under different basicity conditions: A molecular dynamics study. Journal of Molecular Liquids, 336, 116304. https://doi.org/10.1016/j.molliq.2021.116304

68. Ma, S., Li, K., Zhang, J., Jiang, C., Sun, M., Wang, Z., & Bi, Z. (2021b). Effects of CaO and FeO on aluminosilicate melt structure by molecular dynamics simulation. Journal of Molecular Liquids, 325, 115106. https://doi.org/10.1016/j.molliq.2020.115106
69. Ma, W., Zhou, Y., Wei, C., Sheng, M., & Xu, J. (2026). Molecular dynamics study of oxygen network and transport in molten calcium aluminate electrolyte containing FeO and SiO2. Chemical Engineering Science, 333, 124247. https://doi.org/10.1016/j.ces.2026.124247
70. Miao, T., Chen, M., Klemettinen, L., Taskinen, P., & Lindberg, D. (2022). Thermodynamic assessment of FeO-Fe2O3-SiO2 phase equilibria for metallurgical slag applications. Calphad, 79, 102459. https://doi.org/10.1016/j.calphad.2022.102459
71. Mishin, Y. (2021). Machine-learning interatomic potentials for materials science. Acta Materialia, 214, 116980. https://doi.org/10.1016/j.actamat.2021.116980
72. Mukono, T., Wallin, M., & Tangstad, M. (2022). Phase distribution during slag formation in Mn ferroalloy production. Metallurgical and Materials Transactions B, 53, 1122–1135. https://doi.org/10.1007/s11663-022-02441-5
73. Nikolic, S., Hayes, P. C., & Jak, E. (2010). Phase equilibria in the FeO-Fe2O3-SiO2-CaO system under controlled oxygen partial pressure. Metallurgical and Materials Transactions B, 41, 1179–1190. https://scholar.google.com/scholar?q=%22Phase+equilibria+in+the+FeO-Fe2O3-SiO2-CaO+system+under+controlled+oxygen+partial+pressure%22
74. Nikolic, S., Hayes, P. C., & Jak, E. (2011). Liquidus and spinel equilibria in iron silicate slags relevant to nonferrous smelting. Metallurgical and Materials Transactions B, 42, 458–469. https://scholar.google.com/scholar?q=%22Liquidus+and+spinel+equilibria+in+iron+silicate+slags+relevant+to+nonferrous+smelting%22
75. Nikolic, S., Hayes, P. C., & Jak, E. (2012). Effect of CaO on phase equilibria of FeOx-SiO2 slags at controlled oxygen potentials. Metallurgical and Materials Transactions B, 43, 1368–1378. https://scholar.google.com/scholar?q=%22Effect+of+CaO+on+phase+equilibria+of+FeOx-SiO2+slags+at+controlled+oxygen+potentials%22
76. Otis, R. A., & Liu, Z.-K. (2017). pycalphad: CALPHAD-based computational thermodynamics in Python. Journal of Open Research Software, 5, 1. https://doi.org/10.5334/jors.140
77. Park, J. H., & Park, G. H. (2012). Sulfide capacity of CaO-SiO2-MnO-Al2O3-MgO slags at 1873 K. ISIJ International, 52, 764–769. https://scholar.google.com/scholar?q=%22Sulfide+capacity+of+CaO-SiO2-MnO-Al2O3-MgO+slags+at+1873+K%22
78. Paulson, N. H., & Stan, M. (2018). Uncertainty quantification for thermodynamic models and phase diagrams. JOM, 70, 1601-1607. https://scholar.google.com/scholar?q=%22Uncertainty+quantification+for+thermodynamic+models+and+phase+diagrams%22
79. Paulson, N. H., Behera, A., & Stan, M. (2020). Quantifying thermodynamic model uncertainty with Bayesian inference. Calphad, 68, 101728. https://scholar.google.com/scholar?q=%22Quantifying+thermodynamic+model+uncertainty+with+Bayesian+inference%22
80. Paulson, N. H., Jennings, E., & Stan, M. (2019). Bayesian strategies for uncertainty quantification of thermodynamic models. Calphad, 66, 101627. https://scholar.google.com/scholar?q=%22Bayesian+strategies+for+uncertainty+quantification+of+thermodynamic+models%22
81. Pedone, A., Bertani, M., Brugnoli, L., & Pallini, A. (2022). Interatomic potentials for oxide glasses: Past, present, and future. Journal of Non-Crystalline Solids: X, 15, 100115. https://doi.org/10.1016/j.nocx.2022.100115
82. Pedraza, J., Andersson, J.-O., & Sundman, B. (2021). Data-driven strategies for thermodynamic database assessment and optimization. Calphad, 74, 102310. https://scholar.google.com/scholar?q=%22Data-driven+strategies+for+thermodynamic+database+assessment+and+optimization%22
83. Peng, L., Jiang, Z., & Geng, X. (2020). Design of ESR slag for remelting 9CrMoCoB steel through experiments and thermodynamic calculations. Calphad, 70, 101782. https://doi.org/10.1016/j.calphad.2020.101782
84. Pereira, A. C. (2026a). Ca–Al metallothermic reduction: A critical review of reductant design, reaction pathways, slag engineering, and scale-up. Journal International Review of Research Studies, 1(9), 1–49. https://doi.org/10.66104/bn5j2634
85. Pereira, A. C. (2026b). From upgraded titanium slag to modern metallurgical slag engineering: Technologies, industrial applications, and readiness—A critical review. International Journal of Current Science Research and Review, 9(8), 4556–4584. https://doi.org/10.5281/zenodo.22023255

86. Pereira, A. C. (2026c). From Vanadium–Titanium Magnetite to Fe–C–V Alloys: A Critical Review of Vanadium-Bearing Pig Iron Production, Vanadium Partitioning, Refining, and Metallurgical Applications. Journal International Review of Research Studies, 1(09 - September), 1–48. https://doi.org/10.66104/qa1tk476
87. Pereira, A. C. (2026d). Liquid-metal droplet coalescence in metallurgical slags: A critical review of interfacial phenomena, slag properties, hydrodynamics, kinetics, and metal recovery. International Journal of Research and Innovation in Social Science, 10(7), 15007–15036. https://doi.org/10.47772/IJRISS.2026.100701023
88. Pereira, A. C. (2026e). Slag composition control indices in high-temperature metallurgy: A critical review of viscosity, conductivity, corrosion, and refractory wear. Journal International Review of Research Studies, 1(4). https://doi.org/10.66104/7x5etg23
89. Rozario, A., Mukhopadhyay, A., Haidar, S. W., & Hazra, S. (2023). Thermodynamic model of steelmaking slag to reduce refractory consumption during the CONA RC process. Ironmaking & Steelmaking, 50, 1130–1141. https://doi.org/10.1080/03019233.2023.2203010
90. Sajid, M., Bai, C., Yu, W., You, Z., Tan, M., & Aamir, M. (2020). First-principles study of electronic structural and physical properties of CaO-SiO2-Al2O3 ternary slag system by ab initio molecular and lattice dynamics. Journal of Non-Crystalline Solids, 550, 120384. https://doi.org/10.1016/j.jnoncrysol.2020.120384
91. Shapeev, A. V. (2016). Moment tensor potentials: A class of systematically improvable interatomic potentials. Multiscale Modeling & Simulation, 14, 1153–1173. https://doi.org/10.1137/15M1054183
92. Shishin, D., Hidayat, T., Jak, E., & Decterov, S. A. (2013). Thermodynamic optimization of oxide systems using the modified quasichemical model. Calphad, 41, 160–179. https://scholar.google.com/scholar?q=%22Thermodynamic+optimization+of+oxide+systems+using+the+modified+quasichemical+model%22
93. Sineva, S., Fallah-Mehrjardi, A., Hidayat, T., Hayes, P. C., & Jak, E. (2020b). Experimental study of the individual effects of Al2O3, CaO, and MgO on gas/slag/matte/spinel equilibria in the Cu-Fe-O-S-Si-Al-Ca-Mg system at 1473 K and p(SO2)=0.25 atm. Journal of Phase Equilibria and Diffusion, 41, 859–869. https://doi.org/10.1007/s11669-020-00847-9
94. Sineva, S., Fallah-Mehrjardi, A., Hidayat, T., Shevchenko, M., Shishin, D., Hayes, P. C., & Jak, E. (2020a). Experimental investigation of gas/slag/matte/tridymite equilibria in the Cu-Fe-O-S-Si-Al-Ca-Mg system in a controlled gas atmosphere. Journal of Phase Equilibria and Diffusion, 41, 243–256. https://doi.org/10.1007/s11669-020-00810-8
95. Sineva, S., Hayes, P. C., & Jak, E. (2021). Experimental study of the slag/matte/metal/tridymite equilibria in the Cu-Fe-O-S-Si-(Ca) system at 1473 K: Effect of Ca. Metallurgical and Materials Transactions B, 52, 2163–2170. https://doi.org/10.1007/s11663-021-02188-5
96. Sineva, S., Shevchenko, M., Hayes, P. C., & Jak, E. (2022). Transferability of experimentally constrained slag thermodynamics to industrial copper smelting compositions. Metallurgical and Materials Transactions B, 53, 2450–2465. https://scholar.google.com/scholar?q=%22Transferability+of+experimentally+constrained+slag+thermodynamics+to+industrial+copper+smelting+compositions%22
97. Sineva, S., Shishin, D., Shevchenko, M., Hayes, P. C., & Jak, E. (2023). Experimental study of the combined effects of Al2O3, CaO, and MgO on gas/slag/matte/spinel equilibria in the Cu-Fe-O-S-Si-Al-Ca-Mg system. Journal of Sustainable Metallurgy, 9, 599–612. https://doi.org/10.1007/s40831-023-00677-2
98. Song, S., Zhao, J., & Pistorius, P. C. (2020). MgO refractory attack by transient non-saturated EAF slag. Metallurgical and Materials Transactions B, 51, 891–897. https://scholar.google.com/scholar?q=%22MgO+refractory+attack+by+transient+non-saturated+EAF+slag%22
99. Sun, H., Yang, J., & Zhang, R. (2024a). Composition engineering on the structure and transport properties of CaO-SiO2-P2O5: A computational insight. Metallurgical and Materials Transactions B, 55, 1530–1545. https://doi.org/10.1007/s11663-024-03068-4
100. Sun, H., Yang, J., Zhang, R., & Xu, L. (2024b). Insight into the structure and transport properties of the CaO-SiO2-P2O5 system during the phosphorus enrichment process: A molecular dynamics simulation. Journal of Non-Crystalline Solids, 626, 122818. https://doi.org/10.1016/j.jnoncrysol.2023.122818
101. Sun, H., Yang, J., Zhang, T., Li, T., & Zhang, R. (2024c). Insight into TiO2 on transport behavior and heat transfer of CaO-SiO2-FeO-MgO system at different basicities: Molecular dynamics and thermodynamics. Ceramics International, 50, 37589–37606. https://doi.org/10.1016/j.ceramint.2024.07.118
102. Sun, J., Ruzsinszky, A., & Perdew, J. P. (2015). Strongly constrained and appropriately normed semilocal density functional. Physical Review Letters, 115, 036402. https://doi.org/10.1103/PhysRevLett.115.036402
103. Sun, M., Tan, M., Li, T., Li, J., & Shang, B. (2022b). Study on structural properties of refining slags by molecular dynamics simulation with deep learning potential. Journal of Molecular Liquids, 353, 118787. https://doi.org/10.1016/j.molliq.2022.118787

104. Sun, Y., Li, T., Tan, M., & Li, J. (2020a). Effect of CaO on liquid/spinel/matte/gas equilibria in iron-silicate slag systems. Calphad, 69, 101751. https://doi.org/10.1016/j.calphad.2020.101751
105. Sun, Y., Li, T., Tan, M., & Li, J. (2020b). Effect of MgO on phase relations and liquidus behavior of complex metallurgical slags. Calphad, 70, 101803. https://doi.org/10.1016/j.calphad.2020.101803
106. Sun, Y., Li, T., Tan, M., & Li, J. (2020c). Phase transformations and phosphorus enrichment behavior of CaO-SiO2-FeO-P2O5 slags. Metallurgical and Materials Transactions B, 51, 2039-2051. https://doi.org/10.1007/s11663-020-01901-0
107. Sun, Y., Tan, M., Li, T., & Li, J. (2021). Effect of slag basicity on dephosphorization behavior and phosphorus enrichment. Metallurgical and Materials Transactions B, 52, 3403-3414. https://doi.org/10.1007/s11663-021-02270-y
108. Sun, Y., Tan, M., Li, T., & Li, J. (2022a). Influence of temperature on dephosphorization and phosphorus enrichment in steelmaking slag. ISIJ International, 62, 1078-1087. https://doi.org/10.2355/isijinternational.ISIJINT-2021-529
109. Sun, Y., Tan, M., Li, T., & Li, J. (2023). Comprehensive evaluation of phosphorus enrichment capacity of steelmaking slags. Metallurgical and Materials Transactions B, 54, 115-126. https://doi.org/10.1007/s11663-022-02674-4
110. Sun, Y., Yang, J., Zhang, R., & Xu, L. (2025). Slag design for low-carbon dephosphorization through structural and thermodynamic descriptors. Journal of Materials Research and Technology, 36. https://doi.org/10.1016/j.jmrt.2025.04.008
111. Sun, Y., Yang, J., Zhang, R., & Xu, L. (2026). Effect of P2O5 on structure and transport properties of metallurgical slags. JOM, 78. https://doi.org/10.1007/s11837-025-08072-w
112. Talapaneni, T., Yedla, N., & Sarkar, S. (2018). Desulfurization characteristics of high-alumina blast furnace slags. Metallurgical Research & Technology, 115, 502. https://scholar.google.com/scholar?q=%22Desulfurization+characteristics+of+high-alumina+blast+furnace+slags%22
113. Tangstad, M., Bublik, S., Haghdani, S., Einarsrud, K. E., & Tang, K. (2021). Slag properties in Mn-ferroalloy production. Metallurgical and Materials Transactions B, 52, 4110–4124. https://doi.org/10.1007/s11663-021-02347-8
114. Thompson, A. P., Swiler, L. P., Trott, C. R., Foiles, S. M., & Tucker, G. J. (2015). Spectral neighbor analysis method for automated generation of quantum-accurate interatomic potentials. Journal of Computational Physics, 285, 316–330. https://doi.org/10.1016/j.jcp.2014.12.018
115. Tian, M., Klemettinen, L., Chen, M., Taskinen, P., Lindberg, D., Tiljander, M., & O'Brien, H. (2025). Phase equilibria and trace-element deportments in Fe-O-Al2O3-SiO2 slags in equilibrium with copper matte. Metallurgical and Materials Transactions B, 56, 2150–2163. https://doi.org/10.1007/s11663-024-03431-5
116. Tian, M., Wan, X., Chen, M., Taskinen, P., Lindberg, D., & Jokilaakso, A. (2022). Phase equilibria of FeOx-SiO2-Al2O3 slags at 1200 °C and pO2=10^-8.6 atm. Calphad, 79, 102502. https://doi.org/10.1016/j.calphad.2022.102502
117. Wang, R., Zhang, B., Liang, Y., Liu, C., & Jiang, M. (2023). Microscopic insight into foaming behavior of CaO-SiO2-Fe2O3-MgO slag. Ceramics International, 49, 17185–17193. https://scholar.google.com/scholar?q=%22Microscopic+insight+into+foaming+behavior+of+CaO-SiO2-FexO-MgO+slag%22
118. Wang, X., Liao, J., Liu, F., Zhao, B., & Wang, N. (2024). Evaluation of FactSage predictions for complex CaO-MgO-SiO2-Al2O3-TiO2 slags. Metallurgical and Materials Transactions B, 55, 1800-1814. https://scholar.google.com/scholar?q=%22Evaluation+of+FactSage+predictions+for+complex+CaO-MgO-SiO2-Al2O3-TiO2+slags%22
119. Wang, X., Wang, N., Liu, F., Liao, J., & Zhao, B. (2025). Application and evaluation of thermodynamic modeling on phase equilibria of the CaO-MgO-SiO2-Al2O3-TiO2 system. Calphad, 90, 102880. https://doi.org/10.1016/j.calphad.2025.102880
120. Wang, Y., Diao, J., Jiang, L., & Xie, B. (2017). Structural role of phosphorus in CaO-SiO2-P2O5 glass and melt. Metallurgical and Materials Transactions B, 48, 1139–1148. https://doi.org/10.1007/s11663-017-0924-x
121. Wang, Z., Li, K., Jiang, C., Zhang, J., & Sun, M. (2021). Effect of Fe/SiO2 ratio on the structure and properties of nickel-matte smelting slag. Metallurgical and Materials Transactions B, 52, 1463–1474. https://doi.org/10.1007/s11663-021-02113-w
122. Wang, Z., Zhang, J., Li, K., Jiang, C., & Sun, M. (2015). Melting and viscosity behavior of SiO2-CaO-Al2O3-B2O3 slags. Steel Research International, 86, 670–677. https://doi.org/10.1002/srin.201400353
123. Wu, T., He, S., Liang, Y., & Wang, Q. (2015). Molecular dynamics simulation of CaO-SiO2 and CaO-Al2O3 slags. Journal of Non-Crystalline Solids, 411, 145–151. https://scholar.google.com/scholar?q=%22Molecular+dynamics+simulation+of+CaO-SiO2+and+CaO-Al2O3+slags%22

124. Wu, T., Wang, Q., Yu, C., & He, S. (2016). Structural and viscosity properties of CaO-SiO2-Al2O3-FeO slags from molecular dynamics. Journal of Non-Crystalline Solids, 450, 23–31. https://scholar.google.com/scholar?q=%22Structural+and+viscosity+properties+of+CaO-SiO2-Al2O3-FeO+slags+from+molecular+dynamics%22
125. Xie, S., & Zhao, B. (2024). Phase equilibrium studies of nonferrous smelting slags: A review. Metals, 14, 278. https://doi.org/10.3390/met14030278
126. Xie, S., Liao, C., & Zhao, B. (2023). Phase equilibrium studies in the system FeO-SiO2-Al2O3-CaO-MgO at 1200 °C and pO2=10^-8 atm. Calphad, 82, 102588. https://doi.org/10.1016/j.calphad.2023.102588
127. Xie, S., Zhao, B., & Liao, C. (2021). Experimental phase equilibria in lead-rich FeO-SiO2-CaO-Al2O3 slags. Metallurgical and Materials Transactions B, 52, 2900–2913. https://scholar.google.com/scholar?q=%22Experimental+phase+equilibria+in+lead-rich+FeO-SiO2-CaO-Al2O3+slags%22
128. Xu, C., Wang, C., Xu, R., Zhang, J., & Jiao, K. (2021). Effect of Al2O3 on viscosity of CaO-SiO2-Al2O3-MgO-Cr2O3 slags. International Journal of Minerals, Metallurgy and Materials, 28, 797-803. https://scholar.google.com/scholar?q=%22Effect+of+Al2O3+on+viscosity+of+CaO-SiO2-Al2O3-MgO-Cr2O3+slags%22
129. Xu, Z., Zhang, Y., Chi, Y., Yang, J., Zang, X., & Kong, L. (2026). Effect of B2O3 on structure of CaO–Al2O3–CaF2–B2O3 molten slag using molecular dynamics simulation. Ironmaking & Steelmaking, 53(3), 451–460. https://doi.org/10.1177/03019233241277359
130. Yang, S., Jin, H., Chen, Z., Zhang, X., He, S., & Wang, Q. (2023). Effect of TiO2 content on the structure of BaO-CaO-Al2O3-TiO2-Li2O slags by molecular dynamics. Journal of Non-Crystalline Solids, 603, 122084. https://doi.org/10.1016/j.jnoncrysol.2022.122084
131. Yang, W., Gao, Z., Li, S., Deng, L., Liang, B., Kong, X., Chen, X., Liu, D., & Yang, B. (2025). Review of molecular dynamics simulation in extraction metallurgy. Computational Materials Science, 258, 114111. https://doi.org/10.1016/j.commatsci.2025.114111
132. Yang, X., Gao, X., Ueda, S., & Kitamura, S.-Y. (2021). Microstructure and viscosity of dephosphorization slags. ISIJ International, 61, 2490–2499. https://doi.org/10.2355/isijinternational.ISIJINT-2021-150
133. Yao, T., He, S., Wu, T., & Wang, Q. (2017). Molecular dynamics simulation of CaO-SiO2-TiO2 fluorine-free mold flux slags. Ironmaking & Steelmaking, 44, 551–558. https://doi.org/10.1080/03019233.2016.1222111
134. Zhang, L., Han, J., Wang, H., Car, R., & E, W. (2018). Deep Potential Molecular Dynamics: A scalable model with the accuracy of quantum mechanics. Physical Review Letters, 120, 143001. https://doi.org/10.1103/PhysRevLett.120.143001
135. Zhang, R., Wang, Z., Meng, Y., Li, K., Jiang, C., & Zhang, J. (2021a). Quantitative characterization of Al coordination in CaO-Al2O3-SiO2 slags by Raman and 27Al MAS-NMR. Journal of Non-Crystalline Solids, 573, 121116. https://scholar.google.com/scholar?q=%22Quantitative+characterization+of+Al+coordination+in+CaO-Al2O3-SiO2+slags+by+Raman+and+27Al+MAS-NMR%22
136. Zhang, S., Zhang, X., Bai, C., Wen, L., & Lv, X. (2013). Effect of TiO2 content on the structure of CaO-SiO2-TiO2 slags by molecular dynamics simulation. ISIJ International, 53, 1131–1137. https://doi.org/10.2355/isijinternational.53.1131
137. Zhang, S., Zhang, X., Peng, H., Wen, L., Qiu, G., Hu, M., & Bai, C. (2014). Structure of CaO-SiO2-Al2O3-TiO2 slags by molecular dynamics and FTIR spectroscopy. ISIJ International, 54, 734–742. https://doi.org/10.2355/isijinternational.54.734
138. Zhang, X., Liu, C., & Jiang, M. (2021b). Role of Na ions in CaO-SiO2-Na2O melts: A molecular dynamics study. ISIJ International, 61, 1389–1395. https://doi.org/10.2355/isijinternational.ISIJINT-2020-635
139. Zhang, X., Liu, C., & Jiang, M. (2021c). Structure of CaO-Al2O3-Na2O slags by molecular dynamics simulation. Metallurgical and Materials Transactions B, 52, 2604–2611. https://doi.org/10.1007/s11663-021-02184-9
140. Zhao, J., Yang, J., Sun, H., Zhou, Z., & Wang, L. (2026a). Atomistic insights into short- and medium-range structure and transport properties of electric arc furnace slag: Role of iron oxide. Chemical Engineering Science, 327, 122943. https://doi.org/10.1016/j.ces.2025.122943
141. Zhao, R., Jia, G., & Yan, W. (2026b). Molecular dynamics study on microstructure, viscosity, and surface tension of steel slag. Metals, 16, 1051. https://doi.org/10.3390/met16091051
142. Zhou, C., Li, J., Wang, S., Ai, L., Chen, Q., & Zhao, D. (2022). Molecular simulation and spectroscopy of aluminosilicate slag structure. Journal of Non-Crystalline Solids, 590, 121706. https://scholar.google.com/scholar?q=%22Molecular+simulation+and+spectroscopy+of+aluminosilicate+slag+structure%22

143. Zhou, C., Li, J., Wang, S., Zhao, J., Ai, L., Chen, Q., Chen, Q., & Zhao, D. (2023). Development of molecular dynamics and research progress in the study of slag. Materials, 16(15), 5373. https://doi.org/10.3390/ma16155373
144. Zhu, Y., Fan, H., Xu, Z., & Wang, R. (2023). Molecular dynamics study of Ti-bearing oxide melt structure and transport properties. Journal of Molecular Liquids, 370, 121010. https://scholar.google.com/scholar?q=%22Molecular+dynamics+study+of+Ti-bearing+oxide+melt+structure+and+transport+properties%22
145. Zuo, H., Liu, W., Xing, X., & Xue, Q. (2021). Viscosity and desulfurization of BaO-bearing blast furnace slags: Structure-property correlation. Metallurgical and Materials Transactions B, 52, 3550–3562. https://scholar.google.com/scholar?q=%22Viscosity+and+desulfurization+of+BaO-bearing+blast+furnace+slags%3A+Structure-property+correlation%22